3828 *Inorg. Chem.* **2010**, *49*, 3828–3835
DOI: 10.1021/ic902563d

Inorganic Chemistry
Article

First Examples of a Modulated Bridging μ_2-1:2κN-Triazine in Double Helical Silver Compounds. Experimental and Theoretical Evidence

M. Pilar Carranza,[†] Blanca R. Manzano,*[,†] Félix A. Jalón,[†] Ana M. Rodríguez,[‡] Lucía Santos,[§] and Miquel Moreno[∥]

[†]*Departamento de Química Inorgánica, Orgánica y Bioquímica, Facultad de Químicas, IRICA,* [‡]*Departamento de Química Inorgánica, Orgánica y Bioquímica, Escuela Técnica Superior de Ingenieros Industriales, and* [§]*Departamento de Química-Física, Facultad de Químicas, Universidad de Castilla-La Mancha, Avda. Camilo José Cela, 10, E-13071 Ciudad Real, Spain, and* [∥] *Departament de Química, Facultat de Ciències, Universitat Autónoma de Barcelona, 08193 Bellaterra, Barcelona, Spain*

Received December 23, 2009

The synthesis of several silver double helices containing bis(3,5dimethylpyrazolyl)-6-(*R*)-*s*-triazine ligands is described. The structure of two of them has been determined by X-ray difraction. Both derivatives represent the first reported examples of a new interaction mode for a triazine ring that involves a triazine N atom bridging two metal centers. Argentophilic contacts are also present. The Ag−N and Ag−Ag interactions have been demonstrated by theoretical studies, which also showed the clear influence of weak interactions with the counteranion and the effect of the symmetry of the triazine substituent. The different donor characters of these substituents allows a modulation of the strength of the bridging Ag−$N_{triazine}$ interaction. Double $\pi-\pi$ stacking, anion$-\pi$ interactions, hydrogen bonds, and hydrophobic effects are observed in an unusual highly symmetrical interpenetrated three-dimensional superstructure.

Introduction

Supramolecular chemistry is one of the hot topics in the chemistry of the 21st century because of its potential applications in numerous areas such as molecular storage, chemosensing, catalysis, and also in electrical, magnetic, and optical devices.[1] The synthesis and properties of supramolecular self-assemblies formed by metal coordination[2] are clearly influenced by the coordination characteristic of the ligands and metals. Besides, the presence of weak interactions may determine the shape of the molecules and the crystal structure.

It has been reported that the 1,3,5-triazine ring constitutes a remarkable unit to generate supramolecular interactions.[3,4] On the one hand, the *s*-triazine ring is a particular aromatic moiety with a very strong electron-deficient character that allows the formation of $\pi-\pi$ stacking and anion$-\pi$ interactions.[3] On the other hand, this ring contains three nitrogen atoms that can give rise to hydrogen bonds[4] and can also coordinate to metal ions.[5] Some cases of bridging

*To whom correspondence should be addressed. E-mail: blanca.manzano@uclm.es. Fax: + 34-926/295318.

(1) (a) Seo, J. S.; Whang, D.; Lee, H.; Jun, S. I.; Oh, J.; Jeon, Y. J.; Kim, K. *Nature* **2000**, *404*, 982–986. (b) Bruce, D. W. *Acc. Chem. Res.* **2000**, *33*, 831–840. (c) Horn, D.; Rieger, J. *Angew. Chem., Int. Ed.* **2001**, *40*, 4330–4361. (d) Eddaoudi, M.; Kim, J.; Rosi, N.; Vodak, D.; Wachter, J.; O'Keefe, M.; Yaghi, O. M. *Science* **2002**, *295*, 469–472. (e) Arunkumar, E.; Chithra, P.; Ajayaghosh, A. *J. Am. Chem. Soc.* **2004**, *126*, 6590–6598.

(2) (a) Lehn, J.-M. In *Supramolecular Chemistry*; VCH: Weinheim, Germany, 1995. (b) *Transition Metals in Supramolecular Chemistry*; Fabbrizza, L., Poggi, A., Eds.; Kluwer Academic: The Netherlands, 1994. (c) *Encyclopedia of Supramolecular Chemistry*; Atwood, J. L., Steed, J. W., Eds.; Marcel Dekker: New York, 2004; Vol. *2*, pp 1231−1269.(d) Blake, A. J.; Champness, N. R.; Hubberstey, P.; Li, W.-S.; Withersby, M. A.; Schröder, M. *Coord. Chem. Rev.* **1999**, *183*, 117–138. (e) Stang, P. J. *Chem.—Eur. J.* **1998**, *4*, 19–27. (f) Mirkin, C. A.; Holliday, B. J. *Angew. Chem., Int. Ed.* **2001**, *40*, 2022–2043. (g) Fujita, M.; Umemoto, K.; Yoshizawa, M.; Fujita, N.; Kusukawa, T.; Biradha, K. *Chem. Commun.* **2001**, 509–518. (h) Greig, L. M.; Philp, D. *Chem. Soc. Rev.* **2001**, *30*, 287–302. (i) Fujita, M.; Oguro, D.; Miyazawa, M.; Oka, H.; Yamaguchi, K.; Ogura, K. *Nature* **1995**, *378*, 469–471.

(3) (a) Gámez, P.; Reedijk, J. *Eur. J. Inorg. Chem.* **2006**, 29–42. (b) Mooibroek, T. J.; Gámez, P. *Inorg. Chim. Acta* **2007**, *360*, 381–404. (c) Yamauchi, Y.; Yoshizawa, M.; Fujita, M. *J. Am. Chem. Soc.* **2008**, *130*, 5832–5833. (d) Ohmori, O.; Kawano, M.; Fujita, M. *CrystEngComm* **2005**, *7*, 255–259.

(4) (a) Mathias, J. P.; Simanek, E. E.; Zerkowski, J. A.; Seto, C. T.; Whitesides, G. M. *J. Am. Chem. Soc.* **1994**, *116*, 4316–4325. (b) Prins, L. J.; Huskens, J.; de Jong, F.; Timmerman, P.; Reinhoudt, D. N. *Nature* **1999**, *398*, 498–502. (c) Sherrington, D. C.; Taskinen, K. A. *Chem. Soc. Rev.* **2001**, *30*, 83–93. (d) Jonkheijm, P.; Miura, A.; Zdanowska, M.; Hoeben, F. J. M.; De Feyter, S.; Schenning, A. P. H. J.; De Schryver, F. C.; Meijer, E. W. *Angew. Chem., Int. Ed.* **2004**, *43*, 74–78. (e) Sauriat-Dorizon, H.; Maris, T.; Wuest, J. D. *J. Org. Chem.* **2003**, *68*, 240–246. (f) Díaz-Ortiz, A.; Elguero, J.; Foces-Foces, C.; de la Hoz, A.; Moreno, A.; Mateo, M. C.; Sánchez-Migallón, A.; Valiente, G. *New J. Chem.* **2004**, *28*, 952–958. (g) Malek, N.; Maris, T.; Simard, M.; Wuest, J. D. *J. Am. Chem. Soc.* **2005**, *127*, 5910–5916. (h) Helzy, F.; Maris, T.; Wuest, J. D. *Cryst. Growth Des.* **2008**, *8*, 1547–1553. (i) Manzano, B. R.; Jalón, F. A.; Soriano, M. L.; Rodríguez, A. M.; de la Hoz, A.; Sánchez-Migallón, A. *Cryst. Growth Des.* **2008**, *8*, 1585–1594.

(5) (a) Bosch, E.; Barnes, C. L. *Inorg. Chem.* **2002**, *41*, 2543–2547. (b) Manzano, B. R.; Jalón, F. A.; Soriano, M. L.; Carrión, M. C.; Carranza, M. P.; Mereiter, K.; Rodríguez, A. M.; de la Hoz, A.; Sánchez-Migallón, A. *Inorg. Chem.* **2008**, *47*, 8957–8971. (c) Bertelli, M.; Ciani, G.; Proserpio, D. M.; Sironi, A. *J. Mater. Chem.* **1997**, *7*, 1271–1276.

 Published on Web 03/16/2010

Scheme 1

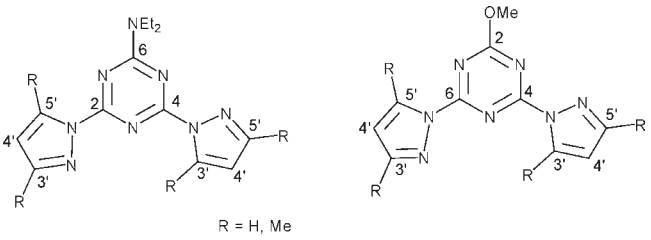

μ_2-1:2κN-heterocyclic systems where a nitrogen atom is bonded to two transition metals have been reported[6] specially with pyridine[7] although the coordination situation has never been theoretically studied. However, only the terminal coordination mode has been observed for the triazine nitrogen atoms. This is probably due to the electron-deficient character of the ring. Considering this fact, we decided to explore the posibility of finding and modulate a bridging coordination of one nitrogen atom to two metallic centers in the *s*-triazine ring. To reach that goal, we synthetized ligands of the type bis(pyrazol-1-yl)-(*R*)-*s*-triazine (Scheme 1) with the aim that the presence of the donor groups, OMe and NEt_2, on the triazine ring will increase the basicity of the N atoms. This basicity could even be modulated by the different donor character of these groups. The existence of the pyrazolyl rings could allow a bisbidentate coordination that would allow the formation of dinuclear complexes with two close metallic centers in the proximity of a N- triazine atom. As metallic center we chose Ag^I because (i) its stereochemical nonrigidity could facilitate the establishment of contacts or interactions; (ii) the ability to exhibit argentophilic interactions[8] could favor the formation of dinuclear derivatives.

Herein, we describe the synthesis of several Ag^I helicoidal compounds featuring a μ_2-1:2κN-triazine unit bridging two silver centers (Scheme 2). This bridging situation is modulated by the donor and geometric characteristic of the triazine substituents. These compounds represent the first examples of this interaction mode for a triazine ring.

Experimental Section

General Procedures. The compounds described below were handled under a nitrogen atmosphere, and air and water were removed completely using the Schlenk techniques. All solvents were freshly distilled under nitrogen, and the reagents were purchased from commercial sources and used without further purification. The preparation of the ligands **1a**,[9] **2a**,[9,10] and **4a**[11] (see Scheme 2) has been described previously. Ligand **3a** is described here for the first time, and an improved method for the synthesis of **4a** is also reported. Elemental analyses were performed with a Thermo Quest FlashEA 1112 microanalyzer. IR spectra were recorded as Nujol mulls with a Perkin-Elmer PE 883 IR (4000−400 cm^{-1}). The FAB^+ mass spectrometry measurements were made with a mass spectrophotometer of magnetic sector Thermo MAT95XP. ^1H, $^{13}C\{^1H\}$, and ^{19}F NMR spectra were recorded on a Varian Unity 300, a Varian Gemini 400, and an Inova 500 spectrometer. Chemical shifts (ppm) are relative to tetramethylsilane (^1H, ^{13}C NMR) and $CFCl_3$ (^{19}F NMR). For $^1H-^{13}C$ gradient-selected heteronuclear multiple quantum and bond coherence (g-HMQC and g-HMBC, respectively) spectra the standard VARIAN pulse sequences were used (VNMR 6.1 C software). The spectra were acquired using 7996 Hz (^1H) and 25133.5 Hz (^{13}C) widths; 16 transients of 2048 data points were collected for each of the 256 increments. See Scheme 1 for the atom numbering. Thermogravimetric analysis (TGA) and differential thermal analysis (DTA) were made with an ATDTG SETARAM apparatus with a 92−16.18 graphite oven and CS32 controller. The analyses were made with a heating rate of 5 °C/ min, under an argon flux in a platinum crucible. N_2 adsorption was measured at 77 K on a Micrometrics Instrument TRISTAR 3000 from the University of Granada. Thermogravimetric analyses have been performed on a Shimadzu TGA-50H instrument using a reactive air atmosphere (rate flow 100 mL min^{-1}) and a heating rate of 20 °C min^{-1} from the University of Granada.

Scheme 2

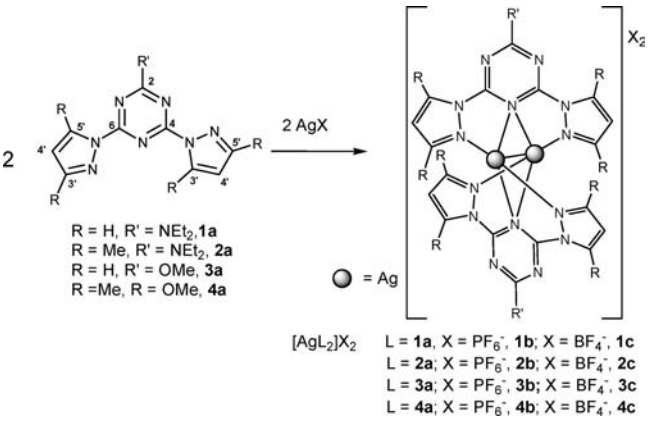

Preparation of 2,4-Bis(pyrazol-1-il)-2-methoxy-1,3,5-triazine, bpzMeOT, 3a. A solution of pyrazole (408.5 mg, 6 mmol) in 20 mL of freshly distilled tetrahydrofuran (THF) was added to a stirred suspension of sodium hydride (60%, 264 mg, 6.6 mmol) in 10 mL of THF. The mixture was stirred at room temperature for 1 h to complete deprotonation. 2,4-Dichloro-2-methoxy-1,3,5-triazine (534 mg, 3 mmol) in 20 mL of THF was added to the above solution. A white precipitate was formed immediately. After being stirred and heating at reflux of THF for 3 h, the solution was evaporated to dryness. The residue was extracted with distilled dichloromethane (20 mL, 4 times). The solvent was removed under vacuum, and the resulting white solid washed with diethyl ether (3 × 15 mL). Yield: 561.9 mg, 77%. ^1H NMR (500 MHz, $CDCl_3$, 25 °C, TMS): δ 8.70 (d, $^3J_{H-H}$ = 2.9 Hz, 2H,

(6) (a) Beringhelli, T.; D'Alfonso, G.; Panigati, M.; Mercandelli, P.; Sironi, A. *Chem.—Eur. J.* **2002**, 5340–5350. (b) Deacon, G. B.; Forsyth, C. M.; Gitlits, A.; Skelton, B. W.; White, A. H. *Dalton Trans.* **2004**, *8*, 1239–1247.

(7) (a) Drew, M. G. B.; Mitchell, P. C. H.; Read, A. R. *J. Chem. Soc. Chem. Commun.* **1982**, 238–239. (b) Bin silong, S.; Kildea, J. D.; Patalinghug, W. C.; Skelton, B. W.; White, A. H. *Aust. J. Chem.* **1994**, *47*, 1545–1551. (c) Bowmaker, G. A.; Effendy; Harvey, P. J.; Healy, P. C.; Skelton, B. W.; White, A. H. *J. Chem. Soc., Dalton Trans.* **1996**, 2459–2465. (d) Effendy; Marcheti, F.; Pettinari, C.; Pettinari, R.; Skelton, B. W.; White, A. H. *Inorg. Chim. Acta* **2007**, *360*, 1414–1423. (e) Di Nicola, C.; Effendy; Marchetti, F.; Pettinari, C.; Skelton, B. W.; White, A. H. *Inorg. Chim. Acta* **2007**, *360*, 1433–1450. (f) Lonnon, D. G.; Craig, D. C.; Colbran, S. B.; Bernhardt, P. V. *Dalton Trans.* **2004**, 778–788. (g) Hannon, M. J.; Painting, C. L.; Plummer, E. A.; Childs, L. J.; Alcock, N. W. *Chem.—Eur. J.* **2002**, *8*, 2225–2238.

(8) (a) Pyykkö, P. *Chem. Rev.* **1997**, *97*, 597–636. (b) Fernández, E. J.; López-de Luzuriaga, J. M.; Monge, M.; Rodríguez, M. A.; Crespo, O.; Gimeno, M. C.; Laguna, A.; Jones, P. G. *Inorg. Chem.* **1998**, *37*, 6002–6006. (c) Zhang, J. P.; Wang, Y. B.; Huang, X. C.; Lin, Y. Y.; Chen, X. M. *Chem.—Eur. J.* **2005**, *11*, 552–561. (d) Streb, C.; Ritchie, C.; Long, D. L.; Körgerler, P.; Cronin, L. *Angew. Chem., Int. Ed.* **2007**, *46*, 7579–7582. (e) Fielden, J.; Long, D-l.; Slawin, A. M. Z.; Kögerler, P.; Cronin, L. *Inorg. Chem.* **2007**, *46*, 9090–9097. (f) Ray, L.; Shaikh, M. M.; Ghosh, P. *Inorg. Chem.* **2008**, *47*, 230–240.

(9) Quiñonero, D.; Deyá, P. M.; Carranza, M. P.; Rodríguez, A. M.; Jalón, F. A.; Manzano, B. R. *Dalton Trans.* **2010**, *39*, 794–806.

(10) Lu, H.-J.; Fan, Y. T.; Gao, J.; Hou, H.-W. *J. Coord. Chem.* **2004**, *57* (8), 693–703.

(11) (a) Yang, C.; Chen, X.-M.; Zhang, W.-H.; Chen, J.; Yang, Y.-S.; Gong, M.-L. *J. Chem. Soc., Dalton Trans.* **1996**, 1767–1768. (b) Yang, C.; Wong, W. T.; Cui, Y.; Yang, Y. *Sci. China, Ser. B: Chem.* **2001**, *44*, 80–92.

H_5), 7.93 (d, $^3J_{H-H}$ = 0.8 Hz, 2H, H_3), 6.57 (dd, 2H, H_4), 4,26 (s, 3H, OCH_3). ^{13}C NMR (500 MHz, $CDCl_3$, 25 °C): δ 173.39 (C_6), 164.28 ($C_{2,4}$), 145.87 ($C_{3'}$), 130.67 ($C_{5'}$), 110,26 ($C_{4'}$), 56.45 (OCH_3). IR (Nujol): $\bar{\nu}$ = 1596, 1564, and 1523 ν(C=N) and ν(C=C). Anal. Calcd for $C_{10}H_9N_7O$: C, 49.38; H, 3.73; N, 40.31. Found: C, 49.23; H, 3.74; N, 40.28.

Preparation of 2,4-Bis(3,5-dimethylpyrazol-1-il)-2-methoxy-1,3,5-triazine, bpz*MeOT, 4a. This ligand was prepared in a similar way to **3a** from 3,5-dimethylpyrazole (576.8 mg, 6 mmol), sodium hydride (60%, 264 mg, 6.6 mmol), and 2,4-dichloro-2-methoxy-1,3,5-triazine (534 mg, 3 mmol) and heating at reflux 16 h. Yield: 727.4 mg, 81%. ^{1}H NMR (500 MHz, $CDCl_3$, 25 °C, TMS): δ 6.08 (s, 2H, $H_{4'}$), 3,49 (s, 3H, O*Me*), 2.74 (s, 6H, $Me_{5'}$), 2.34 (s, 6H, $Me_{3'}$).

Preparation of [Ag$_2$(1a)$_2$](PF$_6$)$_2$, 1b. A solution of **1a** (59.14 mg, 0.208 mmol) in 10 mL of CH_2Cl_2 was added to a solution of $AgPF_6$ (52.59 mg, 0.208 mmol) in 10 mL of CH_2Cl_2. The mixture was stirred for 30 min in the absence of light. The solvent was evaporated, the crude solid was washed with diethyl ether (2 × 5 mL), and an air stable, light-sensitive white solid was obtained (99.44 mg, 89%). ^{1}H NMR (500 MHz, [D$_6$]Acetone, 25 °C, TMS): δ 8.90 (d, $^3J_{H-H}$ = 2.8 Hz, 2H, $H_{5'}$), 7.95 (d, $^3J_{H-H}$ = 1.7 Hz, 2H, $H_{3'}$), 6.77 (dd, 2H; $H_{4'}$), 3.90 (q, $^3J_{H-H}$ = 7.0 Hz, 4H, NCH_2CH$_3$), 1.34 (t, $^3J_{H-H}$ = 7.0 Hz, 6H, NCH$_2$$CH_3$). ^{13}C NMR (500 MHz, [D$_6$]Acetone, 25 °C): δ 164.12 (C_6), 159.80 ($C_{2,4}$), 145.03 ($C_{3'}$), 130.70 ($C_{5'}$), 111.12 ($C_{4'}$), 43.00 (NCH_2CH$_3$), 12.58 (NCH$_2$$CH_3$). ^{19}F NMR (500 MHz, [D$_6$]Acetone, 25 °C): δ −73.1 (d, $^1J_{P-F}$ = 708.0 Hz, PF_6). IR (Nujol): $\bar{\nu}$ = 1621, 1602, and 1511 ν(C=N) and ν(C=C); 849 (ν(PF)) and 557 cm^{-1} (δ(PF)). MS (FAB)$^+$: *m*/*z* (%) 675 (8.8) [AgL$_2$]$^+$, 500 (1.6) [Ag$_2$L]$^+$, 391 (100) [AgL]$^+$. Anal. Calcd for $C_{22}H_{24}Ag_2F_{12}N_{16}P_2$: C, 25.95; H, 2.38; N, 22.01. Found: C, 25.74; H, 2.32; N, 21.83.

Preparation of [Ag$_2$(1a)$_2$](BF$_4$)$_2$, 1c. A similar procedure to that of **1b** was employed using 40.49 mg (0.208 mmol) of $AgBF_4$ and obtaining compound **1c** as an air stable, light-sensitive white solid (85.61 mg, 86%). ^{1}H NMR (500 MHz, [D$_6$]Acetone, 25 °C, TMS): δ 8.86 (d, $^3J_{H-H}$ = 2.8 Hz, 2H, $H_{5'}$), 7.90 (d, $^3J_{H-H}$ = 1.8 Hz, 2H, $H_{3'}$), 6.74 (dd, 2H, $H_{4'}$), 3.92 (q, $^3J_{H-H}$ = 7.0 Hz, 4H, NCH_2CH$_3$), 1.34 (t, $^3J_{H-H}$ = 7.0 Hz, 6H, NCH$_2$$CH_3$). ^{13}C NMR (500 MHz, [D$_6$]Acetone, 25 °C): δ 164.05 (C_6), 159.82 ($C_{2,4}$), 145.03 ($C_{3'}$), 130.61 ($C_{5'}$), 110.71 ($C_{4'}$), 43.07 (NCH_2CH$_3$), 12.60 (NCH$_2$$CH_3$). ^{19}F NMR (500 MHz, $CDCl_3$, 25 °C): δ −153.4 (s, BF_4). IR (Nujol): $\bar{\nu}$ = 1613, 1595, and 1503 ν(C=N) and ν(C=C); 1050 (ν(BF)) and 521 cm^{-1} (δ(BF)). MS (FAB)$^+$: *m*/*z* 871 (1.4) [Ag$_2$L$_2$X]$^+$, 675 (6.3) [AgL$_2$]$^+$, 500 (2.3) [Ag$_2$L]$^+$, 391 (100) [AgL]$^+$. Anal. Calcd for $C_{22}H_{24}Ag_2B_2F_8N_{16}$: C, 29.30; H, 2.68; N, 24.85. Found: C, 29.45; H, 3.02; N, 24.52.

Preparation of [Ag$_2$(2a)$_2$](PF$_6$)$_2$, 2b. This compound was obtained following the same methodology described for complex **1b** using **2a** (70.81 mg, 0.208 mmol) and $AgPF_6$ (52.59 mg, 0.208 mmol). An air stable, light-sensitive white solid was obtained (106.12 mg, 86%). ^{1}H NMR (500 MHz, $CDCl_3$, 25 °C, TMS): δ 6.13 (s, 2H, $H_{4'}$), 3.75 (q, $^3J_{H-H}$ = 6.8 Hz, 4H, NCH_2-CH$_3$), 2.74 (s, 6H, $Me_{5'}$), 1.91 (s, 6H, $Me_{3'}$), 1.27 (t, $^3J_{H-H}$ = 6.7 Hz, 6H, NCH$_2$$CH_3$). ^{13}C NMR (500 MHz, $CDCl_3$, 25 °C): δ 163.90 (C_6), 161.44 ($C_{2,4}$), 153.43 ($C_{3'}$), 146.16 ($C_{5'}$), 111.69 ($C_{4'}$), 43.53 (NCH_2CH$_3$), 15.66 ($Me_{5'}$), 14.47 ($Me_{3'}$), 12.85 (NCH$_2$$CH_3$). ^{19}F NMR (500 MHz, $CDCl_3$, 25 °C): δ −72.6 (d, $^1J_{P-F}$ = 708.0 Hz, PF_6). IR (Nujol): $\bar{\nu}$ = 1614, 1593, and 1506 ν(C=N) and ν(C=C); 841 (ν(PF)) and 557 cm^{-1} (δ(PF)). MS (FAB)$^+$: *m*/*z* (%) 896 (0.2) [Ag$_2$L$_2$]$^+$, 789 (9.7) [AgL$_2$]$^+$, 556 (0.5) [Ag$_2$L]$^+$, 447 (100) [AgL]$^+$. Anal. Calcd for $C_{34}H_{48}Ag_2F_{12}N_{16}P_2$: C, 34.42; H, 4.08; N, 18.89. Found: C, 34.04; H, 3.79; N, 18.62. Single uncolored crystals suitable for X-ray diffraction were grown from a solution in CH_2Cl_2/hexane at room temperature. The crystalline material is not soluble in acetone or chloroform. The presence of hexane was confirmed after a ^{1}H NMR spectrum in [D$_6$]DMSO. ^{1}H NMR (500 MHz, [D$_6$]DMSO, 25 °C, TMS): δ 6.31 (s, 4H, $H_{4'}$), 3.66 (q, $^3J_{H-H}$ = 7.0 Hz, 8H, NCH_2CH$_3$), 2.68 (s, 12H, $Me_{5'}$), 2.08 (s, 12H, $Me_{3'}$), 1.23 (t, $^3J_{H-H}$ = 7.0 Hz, 13H, NCH$_2$$CH_3$ + CH$_3$-(CH_2)$_4$CH$_3$), 0.86 (m, 1H, CH_3(CH_2)$_4$$CH_3$). There is 4.16% of hexane per dimer.

Preparation of [Ag$_2$(2a)$_2$](BF$_4$)$_2$, 2c. A similar procedure to that of **2b** was employed using 40.49 mg (0.208 mmol) of $AgBF_4$ and obtaining compound **2c** in 80% yield (89.04 mg). ^{1}H NMR (500 MHz, $CDCl_3$, 25 °C, TMS): δ 6.12 (s, 2H, $H_{4'}$), 3.73 (q, $^3J_{H-H}$ = 6.9 Hz, 4H, NCH_2CH$_3$), 2.74 (s, 6H, $Me_{5'}$), 1.92 (s, 6H, $Me_{3'}$), 1.33 (t, $^3J_{H-H}$ = 6.9 Hz, 6H, NCH$_2$$CH_3$). ^{13}C NMR (500 MHz, $CDCl_3$, 25 °C): δ 163.96 (C_6), 161.48 ($C_{2,4}$), 153.28 ($C_{3'}$), 145.93 ($C_{5'}$), 111.72 ($C_{4'}$), 43.47 (NCH_2CH$_3$), 15.69 ($Me_{5'}$), 14.40 ($Me_{3'}$), 12.94 (NCH$_2$$CH_3$). ^{19}F NMR (500 MHz, $CDCl_3$, 25 °C): δ −152.4 (s, BF_4). IR (Nujol): $\bar{\nu}$ = 1618, 1590, and 1504 ν(C=N) and ν(C=C); 1057 (ν(BF)) and 520 cm^{-1} (δ(BF)). MS (FAB)$^+$: *m*/*z* 983 (3.4) [Ag$_2$L$_2$X]$^+$, 896 (0.5) [Ag$_2$L$_2$]$^+$, 789 (6.7) [AgL$_2$]$^+$, 447 (100) [AgL]$^+$. Anal. Calcd for $C_{34}H_{48}Ag_2B_2F_8N_{16}$: C, 38.16; H, 4.52; N, 20.94. Found: C, 38.01; H, 4.59; N, 20.88.

Preparation of [Ag$_2$(3a)$_2$](PF$_6$)$_2$, 3b. This compound was obtained following the same methodology described for complex **1b** using 50.59 mg (0.208 mmol) of **3a** and 52.59 mg (0.208 mmol) of $AgPF_6$. **3b** was obtained as an air stable, light-sensitive white solid (85.64 mg, 83%). ^{1}H NMR (500 MHz, [D$_6$]Acetone, 25 °C, TMS): δ 8.91 (d, $^3J_{H-H}$ = 2.9 Hz, 2H, $H_{5'}$), 7.98 (d, $^3J_{H-H}$ = 1.6 Hz, 2H, $H_{3'}$), 6.81 (dd, 2H, $H_{4'}$), 4.32 (s, 3H, O*Me*). ^{19}F NMR (500 MHz, [D$_6$]Acetone, 25 °C): δ −73.8 (d, $^1J_{P-F}$ = 708.0 Hz, PF_6). IR (Nujol): $\bar{\nu}$ = 1596, 1567, and 1525 (C=N and C=C); 840 (ν(PF)) and 558 (δ(PF)). MS (FAB)$^+$: *m*/*z* (%): 702 (0.6) [Ag$_2$L$_2$]$^+$, 459 (2.5) [Ag$_2$L]$^+$, 350 (100) [AgL]$^+$. Anal. Calcd for $C_{20}H_{18}Ag_2F_{12}N_{14}O_2P_2$: C, 24.21; H, 1.83; N, 19.76. Found: C, 24.10; H, 1.99; N, 19.67.

Preparation of [Ag$_2$(3a)$_2$](BF$_4$)$_2$, 3c. This compound was obtained following the same methodology described for complex **3b** using 40.49 mg (0.208 mmol) of $AgBF_4$. **3c** was obtained as an air stable, light-sensitive white solid (71.95 mg, 79%). ^{1}H NMR (500 MHz, [D$_6$]Acetone, 25 °C, TMS): δ 8.88 (d, $^3J_{H-H}$ = 2.8 Hz, 2H, $H_{5'}$), 8.02 (d, $^3J_{H-H}$ = 1.5 Hz, 2H, $H_{3'}$), 6.80 (dd, 2H, $H_{4'}$), 4.30 (s, 3H, O*Me*). ^{19}F NMR (500 MHz, [D$_6$]acetone, 25 °C): δ −152.4 (s, BF_4). IR (Nujol): $\bar{\nu}$ = 1599, 1570, and 1528 (C=N and C=C); 1061 (ν(BF)) and 521 (δ(BF)). MS (FAB)$^+$: *m*/*z* (%): 702 (1.0) [Ag$_2$L$_2$]$^+$, 459 (4.6) [Ag$_2$L]$^+$, 350 (100) [AgL]$^+$. Anal. Calcd for $C_{20}H_{18}Ag_2B_2F_8N_{14}O_2$: C, 27.43; H, 2.07; N, 22.39. Found: C, 27.32; H, 2.15; N, 22.31.

Preparation of [Ag$_2$(4a)$_2$](PF$_6$)$_2$, 4b. This compound was obtained following the same methodology described for complex **1b** using **4a** (62.26 mg, 0.208 mmol) and $AgPF_6$ (52.59 mg, 0.208 mmol). **4b** was obtained as an air stable, light-sensitive white solid (105.66 mg, 92%). ^{1}H NMR (500 MHz, $CDCl_3$, 25 °C, TMS): δ 6.10 (s, 2H, $H_{4'}$), 4.19 (s, 3H, O*Me*), 2.78 (s, 6H, $Me_{5'}$), 2.02 (s, 6H, $Me_{3'}$). ^{1}H NMR (500 MHz, [D$_6$]Acetone, 25 °C, TMS): δ 6.32 (s, 2H, $H_{4'}$), 4.21 (s, 3H, O*Me*), 2.80 (s, 6H, $Me_{5'}$), 2.05 (s, 6H, $Me_{3'}$). ^{13}C NMR (500 MHz, [D$_6$]acetone, 25 °C): δ 172.93 (C_2), 164.59 ($C_{4,6}$), 154.27 ($C_{3'}$), 145.62 ($C_{5'}$), 112.61 ($C_{4'}$), 56.32 (OCH_3), 15.37 ($Me_{5'}$), 12.97 ($Me_{3'}$). ^{19}F NMR (500 MHz, $CDCl_3$, 25 °C): δ −72.7 (d, $^1J_{P-F}$ = 708.0 Hz, PF_6). ^{19}F NMR (500 MHz, [D$_6$]Acetone, 25 °C): δ −73.0 (d, $^1J_{P-F}$ = 708.0 Hz, PF_6). IR (Nujol): $\bar{\nu}$ = 1603, 1580, and 1543 (C=N and C=C); 847 (ν(PF)) and 558 (δ(PF)). MS (FAB)$^+$: *m*/*z* (%): 959 (1.5) [Ag$_2$L$_2$X]$^+$, 500 (2.6) [Ag$_2$(L−CH$_3$)]$^+$, 406 (100) [AgL]$^+$. Anal. Calcd for $C_{28}H_{34}Ag_2F_{12}N_{14}O_2P_2$: C, 30.45; H, 3.10; N, 17.76. Found: C, 29.97; H, 2.89; N, 17.56. Recrystallization from a CH_2Cl_2/hexane mixture gave colorless crystals suitable for X-ray analysis.

Preparation of [Ag$_2$(4a)$_2$](BF$_4$)$_2$, 4c. This compound was obtained following the same methodology described for complex **4b** using 40.49 mg (0.208 mmol) of $AgBF_4$. **4c** was obtained as an air stable, light-sensitive white solid (70.12 mg, 77%). ^{1}H NMR (500 MHz, [D$_6$]Acetone, 25 °C, TMS): δ 6.30 (s, 2H, $H_{4'}$), 4.20 (s, 3H, O*Me*), 2.82 (s, 6H, $Me_{5'}$), 2.08 (s, 6H, $Me_{3'}$). ^{13}C NMR (500 MHz, [D$_6$]acetone, 25 °C): δ 172.90 (C_2), 164.61

($C_{4,6}$), 154.00 ($C_{3'}$), 145.72 ($C_{5'}$), 112.45 ($C_{4'}$), 56.25 (OCH_3), 15.43 ($Me_{5'}$), 12.86 ($Me_{3'}$). ^{19}F NMR (500 MHz, [D_6]acetone, 25 °C): δ −153.4 (s, BF_4). IR (Nujol): $\bar{\nu}$ = 1598 and 1550 (C═N and C═C); 1066 (ν(BF)) and 523 (δ(BF)). MS (FAB)$^+$: m/z (%): 702 (9.2) $[Ag_2L_2]^+$, 459 (8.6) $[Ag_2L]^+$, 406 (100) $[AgL]^+$. Anal. Calcd for $C_{28}H_{34}Ag_2B_2F_8N_{14}O_2$: C, 34.04; H, 3.47; N, 19.85. Found: C, 33.92; H, 3.53; N, 19.76.

Crystal Structure Determinations of 2b and 4b. Suitable crystals of **2b** and **4b** were grown from a dichloromethane/hexane mixture. A colorless crystal was mounted in each case in a glass capillary. Intensity data were collected at 180 K on a Bruker X8 APEX II CCD-based diffractometer, equipped with a graphite monochromated MoKα radiation source (λ = 0.71073 Å). Data were integrated using SAINT[12] and an absorption correction was performed with the program SADABS.[13] The structures were solved by direct methods using the SHELXTL package,[14] and refined by full-matrix least-squares methods based on F^2. Hydrogen atoms were placed using a "riding model" and included in the refinement at calculated positions.

Crystal Data for 2b. $C_{40}H_{58}Ag_2F_{12}N_{16}P_2$; M_r:3818.20; cubic, space group $I23$; a = 25.711(1), b = 25.711(1), c = 25.711(1) Å, V = 17116.1(1) Å^3; Z = 12; ρ_{calcd} = 1.425 g/cm^3; data/restraints/parameters: 7614/10/320; GOF: 0.970; final R indices $I > 2\sigma(I)$: R_1 = 0.0598, wR_2 = 0.1740; max/min residual electron density:1.532/−0.666 e Å^{-3}. For **2b**: All non-hydrogen atoms were refined with anisotropic thermal parameters except the carbon atoms for the hexane solvent. The one PF_6^- anion resides delocalized in two voids with some hexane disordered molecules. Because it was difficult to obtain a satisfactory model of the solvent molecules and anion within these voids, the density in the voids was accounted for using the squeeze option in Platon (van der Sluis and Spek, 1990; Spek, 2001). In this case, the contributions of all of the electron density in the void, including the PF_6^- ion, were subtracted from the observed structure factors (this is the reason no positional coordinates for the PF_6^- ion appear in the table of atomic coordinates). Each voids region occupies 446 Å^3 per unit cell, and the electron density removed by this squeeze procedure amounts to 83 electrons per void. The derived quantities (M_r, F(000), μ, and Dx) in the crystal data do not contain the contribution from this disordered solvent. The structure is representative of the sample because several crystals were mounted with the same result.

Crystal Data for 4b. $C_{28}H_{34}Ag_2F_{12}N_{14}O_2P_2$; M_r: 1104.37; orthorhombic, space group $Pbca$; a = 21.377(4), b = 15.457(3), c = 23.839(4) Å, V = 7877(2) Å^3; Z = 8; ρ_{calcd} = 1.862 g/cm^3; data/restraints/parameters: 6939/0/551; GOF: 0.990; final R indices $I > 2\sigma(I)$: R_1 = 0.0589, wR_2 = 0.1408; max/min residual electron density:1.172/−0.647 e Å^{-3}.

Computational Details. The computational level used in this work was obviously determined by the substantial size the molecule examined. All calculations were performed at the DFT level with the Perdew−Burke−Ernzerhof (PBE1PBE) functional[15] as implemented in the Gaussian 03 Rev. D.02 package programs.[16] Effective core potentials (ECPs) were used to represent the innermost electrons of the Ag atom, while its outer electrons were described with the basis set associated with the pseudopotential SDD[16] including f polarization functions. The 6-311G (d,p) basis was used for the rest of the atoms in the system.

Full geometry optimization and direct location of stationary points was carried out by means of the Schlegel gradient optimization algorithm[17] by using redundant internal coordinates

The natural bond orbital (NBO) analysis was carried out with the NBO 3.0 program as implemented in the Gaussian 03. The Wiberg indices[18] were also calculated. The Atoms-In-Molecules (AIM) analysis[19] was performed by using the AIM2000 (version 2.0) program[19,20] with the same level of calculation used to obtain the wave functions from the geometry optimizations of the cations of **2b**, **4b**, **5b**, and **6b** . In AIM the main topological properties of the electron density ρ(r) of a molecule are summarized in terms of its critical points (CPs).

A criterion used to evaluate the nature of the CPs is the sign of the Laplacian of ρ(r) at the bond critical point, $\nabla^2[\rho(r)]$, where a covalent interaction is characterized by a negative value of $\nabla^2[\rho(r)]$ whereas a closed-shell interaction is characterized by $\nabla^2[\rho(r)] > 0$. Hydrogen bonds are well-known examples of a closed-shell interaction.

Results and Discussion

Synthesis and Characterization. Reaction of the pyrazolate salts with the corresponding dichloro-*s*-triazine derivatives gave ligands **1a**−**4a**. Ligand **3a** is described here for the first time, and an improved method for the synthesis of **4a** is also reported that is a modification from that used for the similar ligand with 4-methyl-pyrazole[21] (see Experimental Section). Reaction of **1a**−**4a** with $AgPF_6$ or $AgBF_4$ gave the complexes **1b**−**4b** and **1c**−**4c**, respectively, as air-stable white solids (Scheme 2). We used ligands with non-methylated and methylated pyrazolyl rings because, according to our previous experience,[22] the presence of the methyl groups could increase the solubility of ligands and complexes. This was confirmed experimentally, and we also observed that the ligands with the diethylamino group were more soluble than those containing the methoxi group. In the ^1H−NMR spectra only one type of symmetric ligand is observed, which points to a symmetric structure although the existence of dynamic processes in solution can not be

(12) SAINT+ v7.12a. *Area-Detector Integration Program*. Bruker-Nonius AXS. Madison, Wisconsin, USA, 2004.
(13) Sheldrick, G. M. *SADABS, A Program for Empirical Absorption Correction*, version 2004/1; University of Göttingen: Göttingen, Germany, 2004.
(14) *SHELXTL-NT, Structure Determination Package*, version 6.12; Bruker-Nonius AXS: Madison, WI, 2001.
(15) (a) Perdew, J. P.; Burke, K.; Ernzerhof., M. *Phys. Rev. Lett*. **1996**, *77*, 3865–3868. (b) Perdew, J. P.; Burke, K.; Ernzerhof., M. *Phys. Rev. Lett*. **1997**, *78*, 1396.
(16) Frisch, M. J.; Trucks, G. W.; Schlegel, H. B.; Scuseria, G. E.; Robb, M. A.; Cheeseman, J. R., Jr.; Montgomery, J. A.; Vreven, T.; Kudin, K. N.; Burant, J. C.; Millam, J. M.; Iyengar, S. S.; Tomasi, J.; Barone, V.; Mennucci, B.; Cossi, M.; Scalmani, G.; Rega, N.; Petersson, G. A.; Nakatsuji, H.; Hada, M.; Ehara, M.; Toyota, K.; Fukuda, R.; Hasegawa, J.; Ishida, M.; Nakajima, T.; Honda, Y.; Kitao, O.; Nakai, H.; Klene, M.; Li, X.; Knox, J. E.; Hratchian, H. P.; Cross; J. B.; Bakken, V.; Adamo, C.; Jaramillo, J.; Gomperts, R.; Stratmann, R. E.; Yazyev, O.; Austin, A. J.; Cammi, R.; Pomelli, C.; Ochterski, J. W.; Ayala, P. Y.; Morokuma, K.; Voth, G. A.; Salvador, P.; Dannenberg, J. J.; Zakrzewski, V. G.; Dapprich, S.; Daniels, A. D.; Strain, M. C.; Farkas, O.; Malick, D. K.; Rabuck, A. D.; Raghavachari, K.; Foresman, J. B.; Ortiz, J. V.; Cui, Q.; Baboul, A. G.; Clifford, S.; Cioslowski, J.; Stefanov, B. B.; Liu, G.; Liashenko, A.; Piskorz, P.; Komaromi, I.; Martin, R. L.; Fox, D. J.; Keith, T.; Al-Laham, M. A.; Peng, C. Y.; Nanayakkara, A.; Challacombe, M.; Gill, P. M. W.; Johnson, B.; Chen, W.; Wong, M. W.; Gonzalez, C.; Pople, J. A. *Gaussian 03*, Revision D.02; Gaussian, Inc.: Wallingford, CT, 2004.
(17) Schlegel, H. B. *J. Comput. Chem*. **1982**, *3*, 214–218.
(18) Wiberg, K. B. *Tetrahedron* **1968**, *24*, 1083–1096.
(19) (a) Bader, R. F. W. *Chem. Rev*. **1991**, *91*, 893–928. (b) Bader, R. F. W. *Atoms in Molecules. A Quantum Theory*; Clarendon: Oxford, 1990.
(20) http//www.AIM200.
(21) Gómez de la Torre, F.; de la Hoz, A.; Jalón, F. A.; Manzano, B. R.; Otero, A.; Rodríguez, A. M.; Rodríguez-Pérez, M. C.; Echevarría, A.; Elguero, J. *Inorg. Chem*. **1998**, *37*, 6606–6614.
(22) (a) Carrión, M. C.; Díaz, A.; Guerrero, A.; Jalón, F. A.; Manzano, B. R.; Rodríguez, A. *New J. Chem*. **2002**, *2*, 305–312. (b) Manzano, B. R.; Jalón, F. A.; Ortiz, I. M.; Soriano, M. L.; Gómez de la Torre, F.; Elguero, J.; Maestro, M. A.; Mereiter, K.; Claridge, T. D. W. *Inorg. Chem*. **2008**, *47*, 413–428.

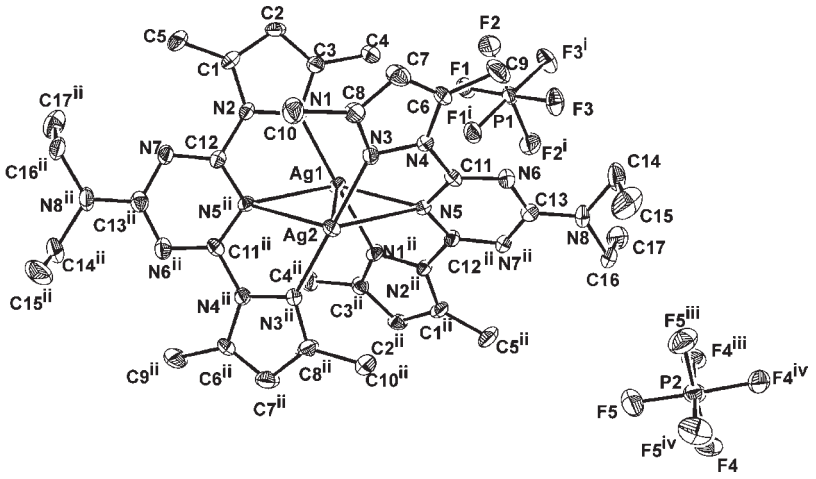

Figure 1. ORTEP representation of complex **2b** (ellipsoids at 30% level). Symmetry transformations used to generate equivalent atoms: i, $x, -y+1, -z$; ii, $-x+1, -y+1, z$; iii, $-y+1, z, -x+1$.

excluded considering the lability of the Ag−N bonds.[5b,23] Changes in the chemical shifts with respect to the free ligands are observed, specially in the Me^3 of the pyrazolyl groups. The presence of the counteranions was confirmed by ^{19}F-NMR and the IR spectra (see Experimental Section). In the FAB-MS spectra peaks corresponding to the fragments $[AgL]^+$, $[Ag_2L]^+$, $[AgL_2]^+$, $[Ag_2L_2]^+$, or $[Ag_2L_2X]^+$ have been observed, a fact that points to the presence of dinuclear derivatives.

We obtained crystals suitable for an X-ray diffraction study in the case of two methylated derivatives, **2b** and **4b**, both containing the hexafluorophosphate anion. The X-ray diffraction analysis revealed that these compounds have double helical structures formed by two ligands that bridge two silver ions through the two pyrazolyl rings and a bridging triazine nitrogen atom of each ligand exhibiting an interaction with both silver centers. Besides, argentophilic interactions between the two metallic centers are present. In the crystal studied of **2b** the network only contains the *P* helices whereas in **4b** both enantiomers are present.

The corresponding Oak Ridge thermal ellipsoid plot (ORTEP) representations are reflected in Figures 1 and 2, and a selection of bond distances and angles is gathered in Tables 1 and 2. The asymmetric unit for **2b** contains half a molecule of the compound. The two Ag atoms are contained in a crystallographic C_2 axis making equivalent both ligands. In **4b** the two ligands are different. In both complexes (Figures 1−2 and Tables 1−2) the silver ions could be considered as tetracoordinated in a very distorted tetrahedral environment (τ_4 = 0.50 and 0.52 for **2b** and 0.46 and 0.58 for **4b**, seesaw geometry)[24] generated by two bonds with the pyrazolyl nitrogen atoms of two different ligands and by two longer contacts with one nitrogen atom of each triazine ring, N_{Tz} (N_{Tz}−Ag distances in the range 2.6−2.8 Å, see Tables 1 and 2). In **2b** a nearly

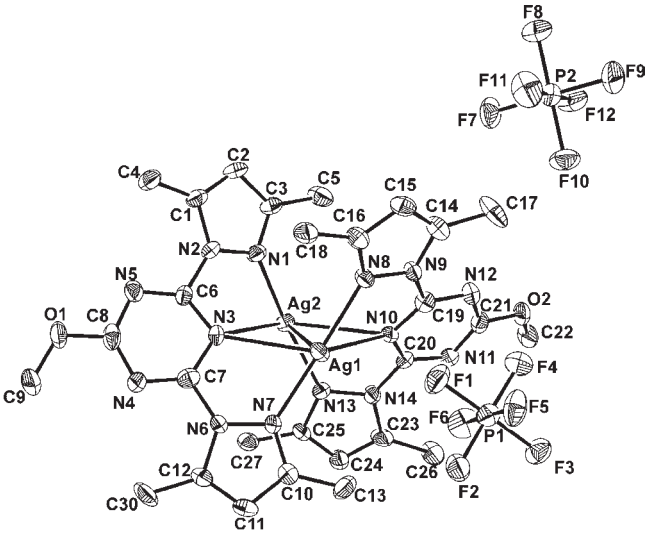

Figure 2. ORTEP representation of complex **4b** (ellipsoids at 30% level).

Table 1. Selected Bond Distances and Angles for **2b**

Ag(2)−N(5)	2.674(4)	Ag(1)−N(5)	2.634(4)
Ag(2)−N(3)	2.132(5)	Ag(1)−N(1)	2.125(4)
Ag(1)−Ag(2)	2.9082(8)		
Ag(2)−Ag(1)−N(5)	57.4(1)	N(1)−Ag(1)−N(5)^i	68.7(2)
Ag(1)−Ag(2)−N(5)	56.1(1)	N(3)−Ag(2)−N(3)^i	175.0(3)
Ag(2)−N(5)−Ag(1)	66.43(2)	N(5)−Ag(2)−N(5)^i	112.3(2)
N(1)−Ag(1)−N(1)^i	174.8(2)	N(3)−Ag(2)−N(5)	110.0(1)
N(5)−Ag(1)−N(5)^i	114.9(2)	N(3)−Ag(2)−N(5)^i	66.9(1)
N(1)−Ag(1)−N(5)	114.3(2)		

^{i} Symmetry transformations used to generate equivalent atoms: $-x+1, -y+1, z$.

symmetrical bridging interaction is found [$(N_{Tz}-Ag2) - (N_{Tz}-Ag1) = \Delta(\mu\text{-}N_{Tz}-Ag) = 0.040$ Å], whereas in **4b** the bridge is not symmetrical [$\Delta(\mu\text{-}N_{Tz}-Ag) = 0.201$ and 0.227 Å]. The angles Ag−Ag−N (Tables 1−2) also reflect the different symmetry of the two complexes. Short intramolecular silver−silver contacts[5a,8] are observed [2.9079(8) and 2.8482(11) Å for **2b** and **4b**, respectively] and these are shorter than the sum of the van der Waals radii[25] (3.44 Å)

(23) (a) Fielden, J.; Long, D.-L.; Slawin, Z.; Kögerler, A. M.; Cronin, L. *Inorg. Chem.* **2007**, *46*, 9090–9097. (b) Reger, D. L.; Semeniuc, R. F.; Smith, M. D. *Eur. J. Inorg. Chem.* **2003**, 3480–3494. (c) Blondeau, P.; van der Lee, A.; Barboiu, M. *Inorg. Chem.* **2005**, *44*, 5649–5693. (d) Chen, C.-L.; Kang, B.-S.; Su, C.-Y. *Aust. J. Chem.* **2006**, *59*, 3–18. (e) Reger, D. L.; Semeniuc, R. F.; Rassolov, V.; Smith, M. D. *Inorg. Chem.* **2004**, *43*, 537–554. (f) Seward, C.; Chan, J.; Song, D.; Wang, S. *Inorg. Chem.* **2003**, *42*, 1112–1120.

(24) Yang, L.; Powell, D. R.; Houser, R. P. *Dalton Trans.* **2007**, 955–964.

(25) Bondi, A. *J. Phys. Chem.* **1964**, *68*, 441–451.

Table 2. Selected Bond Distances and Angles for **4b**

Ag(2)−N(3)	2.878(7)	Ag(1)−N(3)	2.677(1)
Ag(2)−N(10)	2.858(7)	Ag(1)−N(10)	2.631(7)
Ag(2)−N(1)	2.150(7)	Ag(1)−N(7)	2.172(7)
Ag(2)−N(13)	2.148(7)	Ag(1)−N(8)	2.200(7)
Ag(1)−Ag(2)	2.848(1)	Ag(2)−F(12)^{i}	2.921(6)
Ag(2)−Ag(1)−N(3)	62.7(1)	N(7)−Ag(1)−N(3)	66.5(2)
Ag(2)−Ag(1)−N(10)	62.7(1)	N(10)−Ag(1)−N(7)	122.2(2)
Ag(1)−Ag(2)−N(3)	55.7(1)	N(8)−Ag(1)−N(3)	112.5(2)
Ag(1)−Ag(2)−N(10)	54.9(1)	N(1)−Ag(2)−N(13)	169.3(3)
Ag(2)−N(3)−Ag(1)	61.6(1)	N(1)−Ag(2)−N(10)	108.0(2)
Ag(2)−N(10)−Ag(1)	62.3(1)	N(10)−Ag(2)−N(13)	63.2(2)
N(7)−Ag(1)−N(8)	171.1(3)	N(1)−Ag(2)−N(3)	63.4(2)
N(10)−Ag(1)−N(3)	125.2(2)	N(3)−Ag(2)−N(13)	112.7(2)
N(10)−Ag(1)−N(8)	66.0(2)	N(10)−Ag(2)−N(3)	110.5(2)

^{i} Symmetry transformations used to generate equivalent atoms: $x, -y + 1/2 + 1, +z - 1/2$.

Table 3. Parameters for the Anion−π and π−π Stacking Interactions Found in Complexes **2b** and **4b** (see Scheme 3)

Anion−π			
	$d_{\text{F-centr}}$ (Å)	$d_{\text{F-plane}}$ (Å)	β
2b	2.812(1)	2.798(5)	6.1(2)°
4b	2.763(6)	2.727(6)	9.3(2)°

π−π Stacking				
	$d_{\text{centr-centr}}$ (Å)	$d_{\text{centr-plane}}$ (Å)	γ	β
2b	4.226(4)	3.344(5)	37.7(2)°	37.7(2)°

and quite similar to the metal−metal distance in metallic silver (2.884 Å).[26] The two triazine nitrogen atoms involved in the interaction and the silver atoms are coplanar, and the dihedral angles formed by this plane and those of the triazine rings are of 65.9° for **2b** and 57.9 and 60.4° for **4b**. The three rings of each ligand are not coplanar, possibly as a consequence of the double helical structure, and a higher asymmetry is observed again in **4b**. Whereas in **2b** the dihedral angle formed between the triazine and each pyrazolyl ring is about 20°, in **4b** the angles of the central ring with one pyrazole range between 25 and 30° but with the other pyrazole the angle is around 9°.

The crystal packing of **4b** and **2b** is very different, and they crystallize in an orthorhombic or cubic crystal system, respectively. This last system is not usual for such large molecules. For compound **4b**, zigzag chains with anions and the double helices alternating along the *b* axis are formed. Both groups interact through anion−π[27] (Table 3) and Ag−F contacts[28] ($d_{\text{Ag-F}}$ = 2.922(6) Å). In compound **2b**, in spite of the high symmetry of the lattice, the scaffold is quite complex. The crystal structure consists of a 3D 2-fold interpenetrating cubic network supported by weak interactions with nanosized cages inside.[29] Each network is displaced with respect to the other half of the edge in the *x*, *y*, and *z* axes (see Figure 3). The building unit is formed by association of a pair of double-helical molecules linked through double π−π stacking interactions[30] between the pyrazole rings and double anion−π interactions between the triazine rings and the PF_6^- ions situated between the two helices (Figure 3, Table 3, and Scheme 3). These pairs are situated in the middle of the edges of a cube. This scaffold is like an expanded equivalent of the NbO structure where both ions are substituted by the pairs of helices. The anions that are not involved in the formation of the pairs are packed in the lattice through hydrogen bonds (F···H−C distances of 2.39 and 2.54 Å) with six helices. The network formed contains symmetric hydrophobic cavities with an approximate diameter and volume of 12 Å and 940 Å^3, respectively, where disordered hexane molecules are hosted (detected by NMR spectroscopy, and thermogravimetric analysis, see Figure 4 and Supporting Information, Figure S3). In fact, we propose that this special crystalline structure is possibly templated by the hexane molecules because, although the double helical species can be obtained by direct reaction, crystals were not obtained in the absence of hexane. In principle, the presence of these cavities could have applications for gas storage. However, this was not confirmed experimentally. A DGA/DTA experiment was carried out (see Supporting Information, Figure S3). When the sample was heated a mass loss of 2.5% and 0.6% was detected at 160 and 215 °C, respectively, and two narrow endotermic peaks were observed at these temperatures. This mass loss

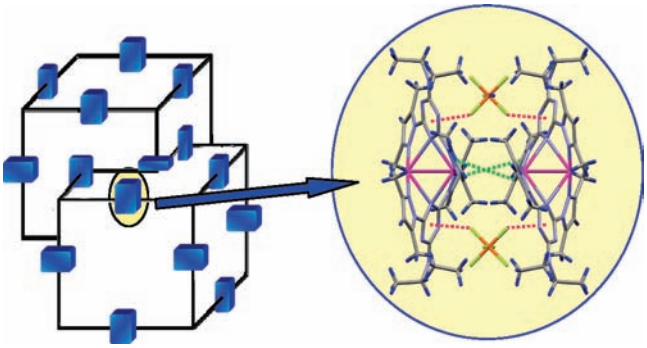

Figure 3. Schematic representation of the interpenetrated structure and detail of the association of two helices in **2b** (dashed pink lines = anion−π, green lines = π−π stacking).

Scheme 3. Schematic Representations of the Anion−π and π−π Stacking Interactions in **2b**[a]

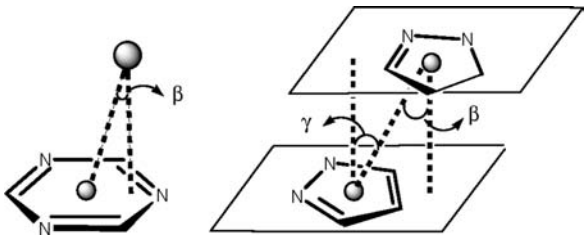

[a] Small circles represent the centroids of the rings.

(26) (a) Greenwood, N. N.; Earnshaw, A. *Chemistry of the Elements*; Pergamon: Oxford, 1984. (b) Pauling, L. *The Nature of the Chemical Bond*, 3rd ed.; Cornell University Press: Ithaca, NY, 1960.

(27) (a) Gamez, P.; Mooibroek, T. J.; Teat, S. J.; Reedijk, J. *Acc. Chem. Res.* **2007**, *40*, 435–444. (b) Schottel, B. L.; Chifotides, H. T.; Dunbar, K. R. *Chem. Soc. Rev.* **2008**, *37*, 68–84.

(28) Mooibroek, T. J.; Black, C. A.; Gamez, P.; Reedijk, J. *Cryst. Growth Des.* **2008**, *8*, 1082–1093.

(29) (a) Niu, C. Y.; Wu, B. L.; Zheng, X. F.; Zhang, H. Y.; Li, Z. J.; Hou, H. W. *Dalton Trans.* **2007**, 5710–5713. (b) Zhang, J. P.; Kitagawa, S. *J. Am. Chem. Soc.* **2008**, *130*, 907–917.

(30) (a) Janiak, C. *Dalton Trans.* **2000**, 3885–3896. (b) Hunter, C. A.; Sanders, J. K. M. *J. Am. Chem. Soc.* **1990**, *112*, 5525–5534. (c) Hunter, C. A. *Chem. Soc. Rev.* **1994**, 101–109. (d) Meyer, E. A.; Castellano, R. K.; Diederich, F. *Angew. Chem., Int. Ed.* **2003**, *42*, 1210–1250.

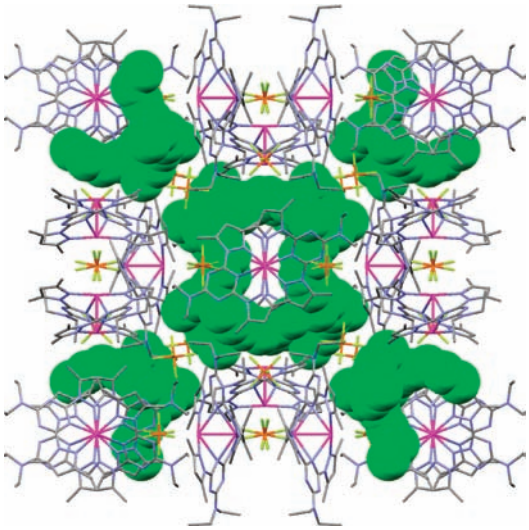

Figure 4. Unit cell of compound **2b** with the hexane molecules, hosted in the hydrophobic cavities, in space-filling mode.

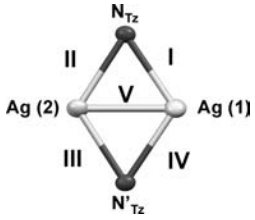

Figure 5. Schematic representation and numbering of the Ag−N and Ag−Ag bonds.

corresponds approximately to the hexane present in **2b**. Above 300 °C, the solid decomposes in a multistep way, first between 327 and 520 °C, with a mass loss that corresponds to the organic ligand and after that, upon 520 °C, a loss corresponding to the counteranion mass, PF_6, is observed. After the loss of hexane the structure collapses, and as consequence the Brunauer−Emmett−Teller (BET) surface, measured at 77 K with N_2 adsorption, is very small (0.3 m^2/g).

Computational Studies. To elucidate the bonding situation in **2b** and **4b**, we carried out a theoretical study at the DFT(BPE1PBE) level. The starting parameters for optimizations were based on the X-ray structure. The calculated molecular geometries and M−M and $M-N_{triazine}$ distances are generally consistent with the experimental X-ray values but with a difference in the type of asymmetry of the triazine bridge in **4b** (Figure 5 and Table 4 and Supporting Information, Figure S4). In the X-ray structure the distances with one silver center are shorter than with the other, whereas in the optimized structure the two metal centers are equivalent, and each one exhibits two Ag−N distances of different length. To explain this difference and considering that in the X-ray structure there is an Ag(2)−F contact (distance of 2.922 Å, Supporting Information, Figure S1) with one of the PF_6^- anions, we optimized the structure with an anion in close proximity to Ag(2). The positions of the fluorine atom that interacts and the phosphorus atoms were fixed to better simulate the experimental situation. The results (Table 4) show a clear influence of the interaction in the sense that the Ag(1)−N distances are shortened while one of the Ag(2)−N distances (**III**) is clearly elongated. Although the distances are not exactly the same as the experimental ones, the situation regarding the two bridges is now more similar. The observed effect of the counteranion reflects the importance that weak interactions may have on the bonding situation and the shape of the molecules.

Table 4. $Ag-N_{Tz}$ and Ag−Ag Distances (Å)

	I	II	III	IV	V
2b[a]	2.634	2.674	2.674	2.634	2.908
2b[b]	2.759	2.761	2.761	2.759	2.899
4b[a]	2.676	2.878	2.859	2.631	2.848
4b[b]	2.879	2.721	2.879	2.721	2.910
4b+PF_6[c]	2.674	2.663	3.004	2.680	2.926
5b[b]	2.846	2.830	2.846	2.830	2.931
6b[b]	2.818	2.734	2.817	2.733	2.893

[a] Experimental data. [b] Theoretical data. [c] Theoretical data including a PF_6^- anion with one F and the P atoms in fixed positions.

Table 5. Bond Orders and Electronic Density at the Bond Critical Points for the Ag−N and Ag−Ag Bonds Evaluated Using the AIM Formalism for the Cations of **2b**, **4b**, [**4b**+PF6], **5b**, and **6b** at the PBE1PBE /6-311G** Level of Theory[a]

		I	II	III	IV	V
2b	BO[b]	0.032	0.032	0.032	0.032	0.029
	$\rho(r)$[c]	0.025	0.025	0.026	0.025	0.026
4b	BO[b]	0.025	0.034	0.025	0.034	0.031
	$\rho(r)$[c]	0.021	0.026	0.021	0.031	0.027
4b+PF_6	BO[b]	0.037	0.038	0.020	0.039	0.032
	$\rho(r)$[c]	0.031	0.028	0.025	0.030	0.027
5b	BO[b]	0.026	0.027	0.026	0.027	0.032
	$\rho(r)$[c]	0.023	0.022	0.022	0.020	0.027
6b	BO[b]	0.028	0.034	0.028	0.034	0.030
	$\rho(r)$[c]	0.023	0.025	0.026	0.025	0.028

[a] See Figure 5 for numbering. [b] Bond order (Wiberg index). [c] Electronic density (in a.u.) at the bond critical point.

To demonstrate the existence of the M−M interaction and the first examples of a μ_2-1:2κ^1N-triazine featuring a bridging interaction mode and also give values for the interaction strength, an NBO analysis was carried out. The calculated Wiberg indexes for the Ag−Ag and $Ag-N_{Tz}$ interactions are gathered in Table 5. These values, similar to those reported for Ag−Ag and Ag−H contacts,[31] are consistent with the existence of the proposed interactions. Furthermore, topological analysis of the charge density using Bader's Atom In Molecules (AIM) theory gave comparable results with all the bonds depicted in Figure 5 being characterized by a bond order critical point (see Table 5 and Figure 6). Analysis of the Laplacian of the electronic density $\nabla^2[\rho(r)]$ also reveals that all these bonds are of the closed-shell type as described in the Computational Details section. As an example the Laplacian of **2b** is shown in the Supporting Information, Figure S6. The same scenario is found for the other studied silver complexes. Finally, we also calculated the Mulliken charges of the Ag and $N_{triazine}$ atoms for the optimized structures of **2b** and the two calculations for **4b** (see Supporting Information, Table S2). On comparing **2b** and **4b**, it is remarkable that while the charge on the silver atoms is similar, the negative charge on the N

(31) (a) Aguado, J. E.; Calhorda, M. J.; Costa, P. J.; Crespo, O.; Félix, V.; Gimeno, M. C.; Jones, P. G.; Laguna, A. *Eur. J. Inorg. Chem.* **2004**, 3038–3047. (b) Liu, C. S.; Chen, P. Q.; Yang, E. C.; Tian, J. L.; Bu, X. H.; Li, Z. M.; Sun, H. W.; Lin, Z. *Inorg. Chem.* **2006**, *45*, 5812–5821.

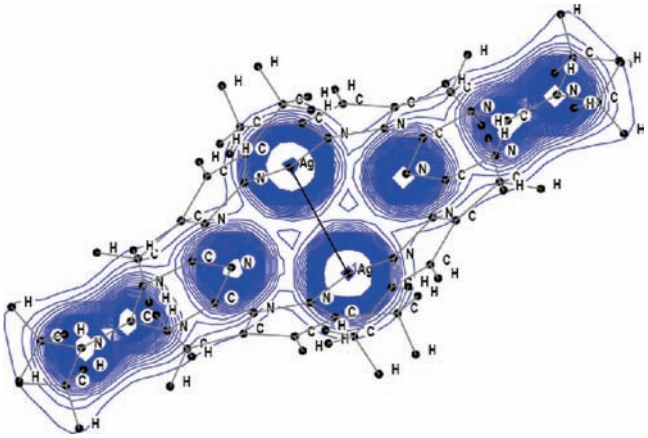

Figure 6. Electronic density in the Ag(1)−Ag(2)−N_{tz} plane for **2b**.

atoms is higher in **2b**, probably reflecting the stronger donor character of the NEt_2 substituent in comparison to OMe.

From the results reported for **2b** and **4b** it can be concluded that the substituent on the triazine ring plays a decisive role on the bonding of this heterocycle. We propose that its donor character is important to modulate the characteristics of the $(Ag)_2-(N_{Tz})_2$ double bridge and that its symmetry is reflected in the symmetry of the bridge. To confirm that, we performed a computational study for the analogous derivatives containing NO_2 (**5b**) or NHEt (**6b**) as substituents. The data of the Ag−N distances are shown in Table 4 and the Wiberg indexes and electronic density are gathered in Table 5. If the sum of the **I**−**IV** distances or the BO orders of these four interactions (Figure 5) is taken as an indication of the strength of the Ag−N_{Tz} interaction, the following order can be deduced from the theoretical results: NEt_2 > NHEt > OMe > NO_2, in agreement with the expectations considering the donor character of the substituents. The experimental results also fit with this sequence. Besides, when the data of **4b** and **4b**+$\mathbf{PF_6}$ are compared in the same way, it is concluded that the presence of the anion reinforces the $(Ag)_2-(N_{Tz})_2$ interaction. On the other hand, the results also reflect that there is a direct relationship between the symmetry of the substituent and the symmetry of the triazine bridge. As expected, the NO_2 derivative (**5b**) exhibit the lowest negative charge on the triazine N atoms (Supporting Information, Table S2).

Conclusion

In summary, we have prepared silver complexes that constitute the first examples of a μ_2-1:2κ^1N-triazine featuring a bridging interaction mode, modulated by the donor character of the triazine substituent. The interactions have been demonstrated by quantum electronic calculations, which also showed the clear influence of weak interactions with the counteranions and the effect of the symmetry of the triazine substituent. Furthermore, an interesting structural framework with a wide variety of weak interactions, possibly templated by the solvent molecules, was found. These weak interactions have proved to be crucial in the construction and design of complex 3D structures.

Acknowledgment. The Spanish Ministry of Science and Innovation (MICINN) and the Junta de Comunidades de Castilla-La Mancha (projects CTQ2008-03783 and PCI08-0054) are acknowledged for financial support.

Supporting Information Available: Figures to complement the X-ray information. TGA/DTA study of **2b**. Optimized structures for the cations of **2b**, **4b**, [**4b**+$\mathbf{PF_6}$], **5b**, and **6b** and the corresponding Cartesian coordinates. Calculated Mulliken atomic charges. Electronic density in the Ag(1)−Ag(2)−N_{Tz} plane for **4b** and [**4b**+$\mathbf{PF_6}$]. Laplacian of the charge density for compound **2b** in the Ag(1)−Ag(2)−N_{Tz} plane. Crystallographic data in CIF format. This material is available free of charge via the Internet at http://pubs.acs.org.